Journal of
Composites Science

MDPI

Article

Electrical Properties of Semiconductor/Conductor Composites: Polypyrrole-Coated Tungsten Microparticles

Jaroslav Stejskal [1,2,*], Marek Jurča [1], Miroslava Trchová [2] and Jan Prokeš [3]

[1] Centre of Polymer Systems, Tomas Bata University in Zlin, 760 01 Zlin, Czech Republic; jurca@utb.cz
[2] Central Laboratories, University of Chemistry and Technology, 166 28 Prague 6, Czech Republic; miroslava.trchova@vscht.cz
[3] Faculty of Mathematics and Physics, Charles University, 180 00 Prague 8, Czech Republic; jan.prokes@matfyz.cuni.cz
* Correspondence: stejskal@utb.cz

Abstract: Tungsten microparticles were coated with globular or nanotubular polypyrrole in situ during the oxidation of pyrrole in aqueous medium with ammonium peroxydisulfate or iron(III) chloride, respectively. The resulting core–shell composites with various contents of tungsten were obtained as powders composed of metal particles embedded in a semiconducting polymer matrix. The coating of tungsten with polypyrrole was analysed by FTIR and Raman spectroscopies. The resistivity of composite powders was determined by the four-point van der Pauw method as a function of pressure applied up to 10 MPa. The degree of compression was also recorded and its relation to electrical properties is discussed on the basis of the percolation concept. The electrical properties of composites are afforded by polypyrrole matrix and they are independent of tungsten content. As the conducting tungsten particles are separated by polypyrrole shells, they cannot produce conducting pathways and behave similarly as a nonconducting filler.

Keywords: core–shell composite; hybrid composite; conducting polymer; conductivity; resistivity under pressure; tungsten microparticles; globular polypyrrole; polypyrrole nanotubes

Academic Editor: Francesco Tornabene

Received: 27 January 2025
Revised: 17 February 2025
Accepted: 19 February 2025
Published: 22 February 2025

Citation: Stejskal, J.; Jurča, M.; Trchová, M.; Prokeš, J. Electrical Properties of Semiconductor/Conductor Composites: Polypyrrole-Coated Tungsten Microparticles. *J. Compos. Sci.* **2025**, *9*, 98. https://doi.org/10.3390/jcs9030098

1. Introduction

Composites are materials composed of at least two solid components that differ in chemical or physical properties and produce separate phases. The morphology of phases and interfacial interactions play a role in their properties that may substantially differ from those of individual components. Composites met in practice are often composed of a filler dispersed in a polymer matrix that provides mechanical and processing properties. While filler is of an inorganic nature, typical polymer phase is organic. In such hybrid composites, the inorganic core–organic shell microstructure is of interest due to the improved interfacial properties that differ from those of simple mixtures.

When working with functional composites, it is usually emphasised that they include a constituent with specific features, e.g., displaying electrical conductivity or magnetism [1–3]. The term of functionality, however, is not limited to these properties. Examples of functional materials are represented by inorganic–organic systems. The organic part often produces a matrix for the dispersion of functional inorganic particulate filler. Inorganic objects coated with an organic substance are a relevant core–shell morphology of such composites. In the next step of design, a polymer matrix can also be functional. This happens in the case of conducting polymers, such as polyaniline or polypyrrole that are redox-active and conducting at a semiconductor level [4,5].

Hybrid organic/inorganic composites have been reported in many studies. Let us limit ourselves to the case when both components are functional in some respects. Polypyrrole, as a representative of organic parts, is an organic conducting polymer with the conductivity of the order of units S cm^{-1} at room temperature in its globular form and one order of magnitude higher, tens S cm^{-1}, for nanotubular morphology. Polypyrrole is a responsive and electroactive polymer, its conductivity of semiconducting character is affected by pH and applied oxidation potential, respectively.

As an example of the functional inorganic part, we can consider tungsten compounds. The literature offers the deposition of polypyrrole at tungsten trioxide [6–9] and tungsten dichalcogenides, viz. tungsten diselenide [10] or the preparation of polypyrrole-coated tungsten disulfide [11–19] or tungsten carbide [20,21]. In all cases, the composites were of the type tungsten compound core/polypyrrole shell with rare exceptions [7].

An interesting combination of polypyrrole with tungsten compounds concerns heteropolyacids, such as silicotungstic and phosphotungstic acid [22]. Unlike dichalcogenides, these acids are well soluble in water, i.e., also in the reaction mixture used for the preparation of polypyrrole. The product is, thus, polypyrrole polycation that produces a salt with tungsten-containing counterions. Such products, however, are not rated as composites.

Some examples of functional behaviour of tungsten composites can be found in the literature. The deposition of tungsten diselenide at polypyrrole yielded an efficient electrocatalyst for water splitting [10], while the reverse strategy, the coating of tungsten disulfide, led to a decrease in catalytic activity in the hydrogen evolution reaction [12]. This was associated with morphology of tungsten compounds and location of catalytic sites at microparticle edges. A photocathode based on polypyrrole/tungsten trioxide was used in hydrogen generation [8]. Polypyrrole/tungsten disulfide was used in a supercapacitor-based sensor [16,18], supercapacitor electrodes [19,23], and as an anode in a sodium-ion battery [11]. Polypyrrole-modified tungsten compounds were applied as a humidity sensor [13], ammonia sensor [7], in vanillin/caffeine detections [16], and in analysis of food and beverages [23]. Polypyrrole/tungsten disulfide was applied for in vivo anticancer drug release [14]. The design of novel thermoelectric composites can also be mentioned [20].

The applications of polypyrrole salts with tungsten heteropolyacids are again mentioned here for the sake of completeness. Polypyrrole doped with silicotungstic acid was a part of composite for an electromagnetic interference shielding [24]. Polypyrrole salts with tungsten heteropolyacid have further been tested for oxygen adsorption on catalytic sites [22] and in photocatalytic removal of pollutant chromium(VI) and organic contaminants [25,26]. The corrosion protection of mild steel by polypyrrole was improved by the introduction of tungstate counterions [23]. Finally, polypyrrole protonated with tungsten heteropolyacid was used in polymer electrolyte membranes for energy storage devices [27].

Unlike tungsten compounds, however, there are no studies on the core–shell composites of polypyrrole with tungsten metal. Tungsten has the highest melting point among metals, 3399 °C, high electrical conductivity, 1.82×10^5 S cm^{-1} (≈25% of that of silver), and thermal conductivity, 175 $Wm^{-1}K^{-1}$ (43% of that of silver) at 20 °C. Tungsten is not ferromagnetic. The present study reports the preparation of composite microparticles with tungsten core and polypyrrole shell. Both globular and nanotubular morphologies of polypyrrole have been considered and compared. The composites of microparticles with metallic conductivity dispersed in a semiconductor matrix are discussed below with respect to their electrical properties.

2. Materials and Methods

2.1. Preparation

Tungsten microparticles of average diameter labelled 5 μm (found D_{50} 1.31 μm) with a broad size distribution and purity of 99.95 wt% were supplied by Nanografi, Ankara, Turkey. Two procedures have been used to prepare core–shell microparticles. The first was the synthesis of globular polypyrrole using ammonium peroxydisulfate (APS) as pyrrole oxidant and the second was the preparation of polypyrrole nanotubes with iron(III) chloride hexahydrate in the presence of methyl orange dye. Various amounts of tungsten powder (2–8 g) were suspended in 100 mL water containing pyrrole. Then, 100 mL aqueous solution of oxidant was added under gentle stirring at room temperature. The 200 mL of reaction mixture contained 0.1 M pyrrole (1.34 g, 20 mmol) and 0.125 M ammonium peroxydisulfate (5.71 g, 25 mmol) in order to obtain globular polypyrrole or 0. 25 M iron(III) chloride hexahydrate (13.5 g, 50 mmol) and 8 mM methyl orange (1.6 mmol, 520 mg), respectively. The polymerisation of pyrrole alone gave 1.404 g of polypyrrole sulfate; the stoichiometric expectation is 1.78 g in a completely protonated form [28]. After 30 min, the tungsten microparticles coated with polypyrrole were separated by filtration and rinsed with water and ethanol to remove any soluble species. The solids were left to dry at ambient temperature in open air for 48 h.

2.2. Characterisation

A scanning electron microscope (Tescan Vega, Brno, Czech Republic) was used to display the morphology. The composite composition was evaluated from the mass increase after pyrrole polymerisation.

ATR FTIR spectra were analysed using a Nicolet 6700 spectrometer (Thermo Nicolet, Waltham, MA, USA) in the 4000–400 cm^{-1} range at a resolution of 4 cm^{-1}, 64 scans, and Happ-Genzel apodization. Raman spectra were registered with a Thermo Scientific DXR Raman microscope (Thermo Fisher Scientific, Waltham, MA, USA) with a 780 nm laser line. The scattered light was analysed by a spectrograph with holographic grating of 400 lines per mm, a pinhole width of 50 μm, and the acquisition time was 10 s with 10 repetitions.

The resistivity of composites was determined using a four-point van der Pauw method with a press operating with a cylindrical glass cell 10 mm in diameter [28]. A current source Keithley 220, a Keithley 2010 multimeter, and a Keithley 705 scanner with a Keithley 7052 matrix card participated in the setup. Powders were compressed with a glass piston carrying four platinum/rhodium electrodes at the perimeter. The resistivity was recorded as a function of applied pressure up to 10 MPa (=102 kp cm^{-2}). It was exerted with an E87H4-B05 stepper motor (Haydon Switch & Instrument Inc., Waterbury, CT, USA) and registered with an L6E3 strain gauge cell (Zemic Europe BV, Etten-Leur, The Netherlands). The sample thickness was monitored during the compression with a dial indicator Mitutoyo ID-S112X (Mitutoyo Corp., Sakado, Japan). The composites could also be compressed at 527 MPa with a manual hydraulic press Trystom H-62 (Trystom, Olomouc, Czech Republic) to free-standing pellets 13 mm in diameter and 1–1.5 mm thick. The conductivity was similarly determined by a routine four-point van der Pauw method.

3. Results and Discussion

3.1. Preparation of Composites

In order to prepare the composites that would combine both moieties to produce inorganic–organic/core–shell microstructures, this is achieved as follows: polypyrrole was prepared by chemical oxidation in acidic aqueous medium (Figure 1). Polypyrrole is obtained as a conducting salt, polypyrrole sulfate. Hydrophobic pyrrole oligomers produced at the early stage of polypyrrole preparation adsorb a dispersed substance, here

tungsten microparticles, and act as initiation sites for the brush-like growth of polymer chains (Figure 2). This concept has been checked in the present study to prepare core tungsten metal microparticles coated with a shell of conducting polypyrrole. Standard polymerisation of pyrrole yields globular morphology. When carried out in the presence of methyl orange dye, polypyrrole nanotubes are produced.

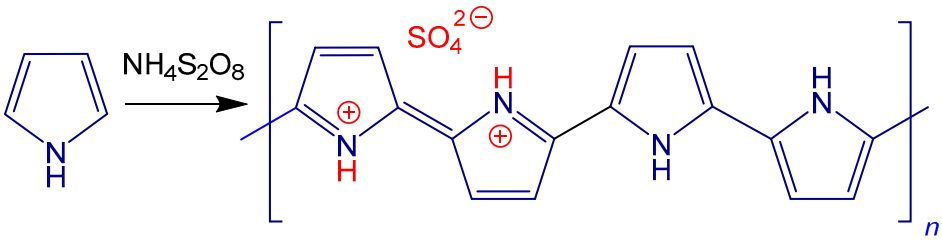

Figure 1. Oxidation of pyrrole with peroxydisulfate in aqueous medium yields polypyrrole sulfate.

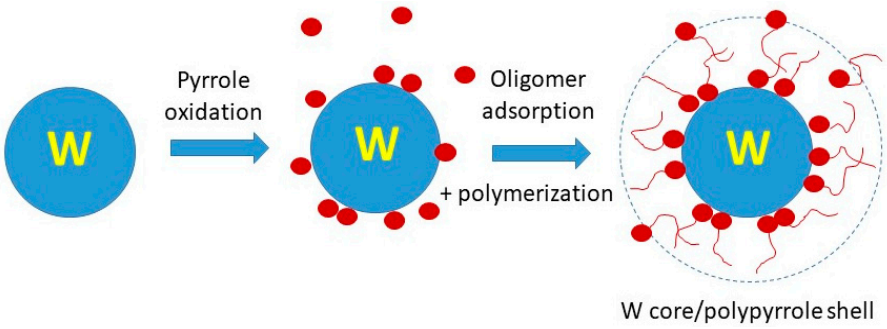

Figure 2. The oxidation of pyrrole in the presence of tungsten microparticles yields pyrrole oligomers at first. They adsorb at tungsten surface and start the growth of polypyrrole chains.

The composition of composites can be calculated from increase in mass after the preparation. Electrical properties are generally dependent on the volume fraction of conducting components. Due to the difference in density of both components, 1.5 g cm^{-3} for polypyrrole and 19.25 g cm^{-3} at 20 °C for tungsten, which is about equal to the density of gold, the volume fractions are considerably lower than weight ones (Table 1).

Table 1. Composite yield, weight fraction of tungsten in the composite, w, and corresponding volume fraction, φ, depending on mass of tungsten entering the preparation, W, in 200 mL of reaction mixture.

W, g	Yield, g	w, wt% W	φ, vol% W
0 (PPy)	1.40	1	1
2	3.40	0.21	0.019
4	5.40	0.74	0.174
6	7.40	0.81	0.240
8	9.40	0.85	0.295

3.2. Morphology

The concept of core–shell morphology is well applicable to microparticles, typically of the order of micrometres size and larger. In the present case, the size of many tungsten microparticles falls below 1 μm (Figure 3). The thickness of polypyrrole coating is estimated with the polyaniline analogy to 100–200 nm. The completeness of the coating can be demonstrated by Raman spectroscopy as well as by microscopy (Figure 4). The last method also illustrates the globular and nanotubular morphology of polypyrrole deposits. A comment is relevant: if the metal particles were still smaller than 100 nm, the reversed

morphology could be observed, i.e., the polypyrrole might be coated with metal particles. This is not the case here.

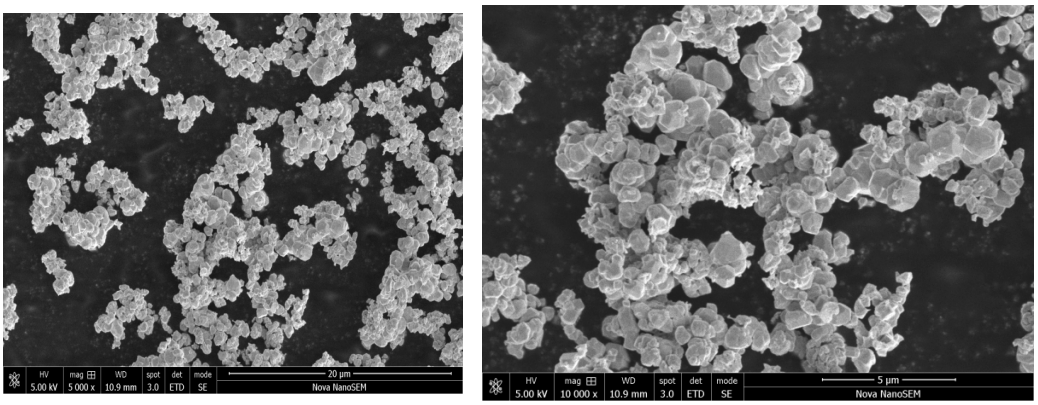

(**a**) (**b**)

Figure 3. Original tungsten microparticles before polypyrrole coating at (**a**) lower and (**b**) higher magnification. Scale bars 20 µm and 5 µm.

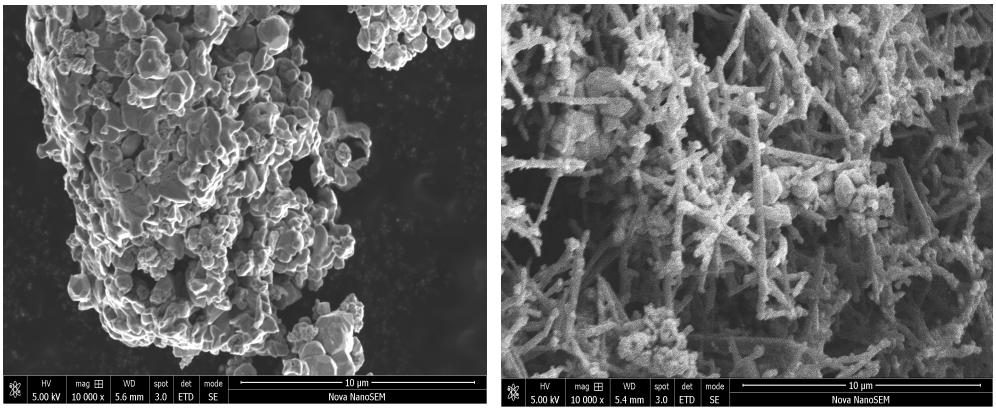

(**a**) (**b**)

Figure 4. Tungsten microparticles with deposited polypyrrole: (**a**) globules and (**b**) nanotubes (4 g of tungsten in 200 mL of reaction mixture). Scale bars 10 µm.

3.3. FTIR Spectra

Infrared spectra of globular polypyrrole/tungsten composites are practically identical with the infrared spectrum of protonated globular polypyrrole regardless of the mass content of tungsten entering the preparation (Figure 5a). They exhibit the main bands, with maxima situated at 1688, 1535, 1452, 1287, 1160, 1092, 1030, 962, 774, and 655 cm^{-1} [29]. The electrical conduction of the samples is associated with the delocalisation of charge carriers over the polypyrrole chain, which manifests itself in the spectra by a broad polaron band at wavenumbers above 2000 cm^{-1}. As expected, the spectrum of tungsten is featureless and does not exhibit any absorption peak. The small shift of the bands for the highest content of tungsten corresponds to the background of its spectrum.

Infrared spectra of polypyrrole nanotubes/tungsten composites are identical with the infrared spectrum of nanotubes alone, regardless of the mass content of tungsten entering the preparation (Figure 5b). They exhibit the bands with maxima situated at 1510, 1430, 1400, 1273, 1123, 1079, 958, 956, 828, 704, and 640 cm^{-1} [29]. The spectra of nanotubular PPy differ from the spectrum of globular PPy; they reflect the presence of methyl orange that acts as a structure-guiding agent.

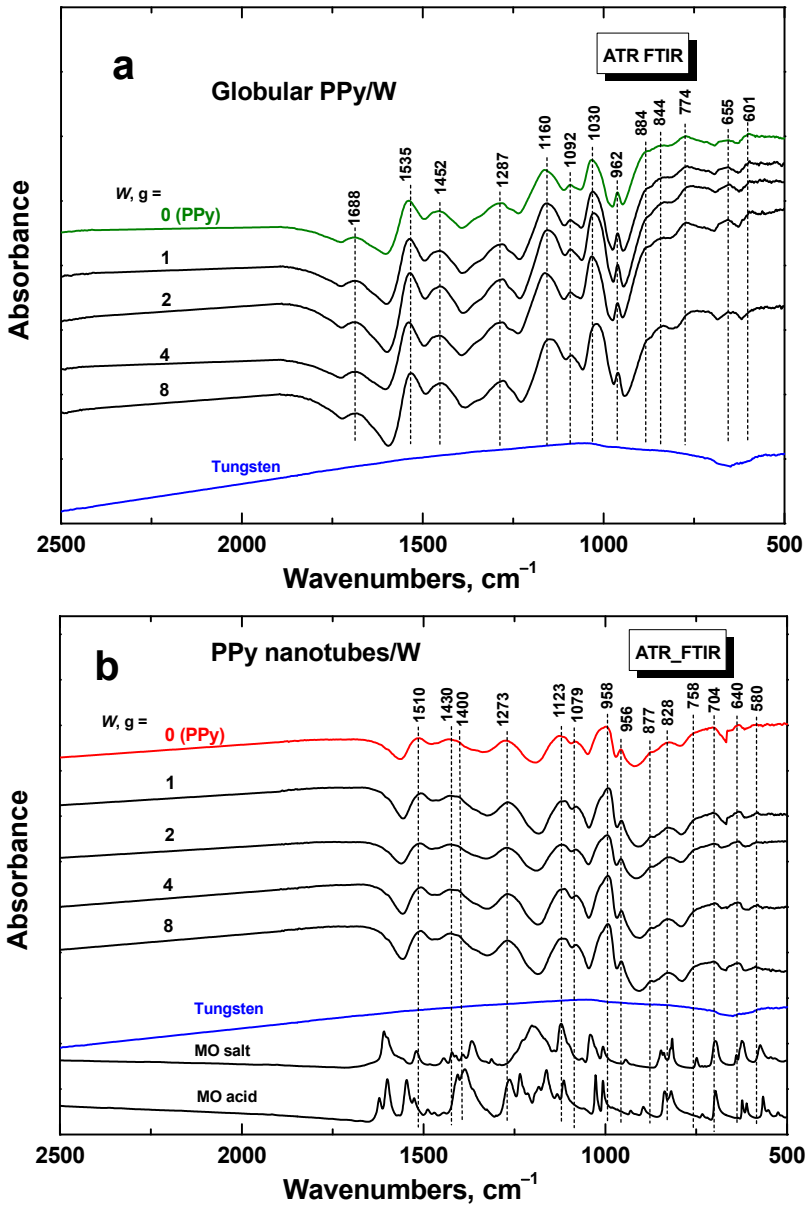

Figure 5. ATR FTIR spectra of (**a**) globular polypyrrole/tungsten composites and (**b**) a composite with polypyrrole nanotubes depending on mass of tungsten entering the preparation, *W*, per 200 mL of reaction mixture. MO stands for methyl orange dye [29].

3.4. Raman Spectra

Raman spectra of globular polypyrrole/tungsten composites dependent on tungsten mass entering the preparation are very close to the spectrum of protonated globular polypyrrole (Figure 6a). The maxima of the bands detected in the spectra are situated at 1589, 1470, 1375, 1310, 1239, 1087, 1047, and 930 cm^{-1} [30]. The bands of the Raman spectrum of tungsten are not observed in the spectra of composites. This confirms that the tungsten particles are well coated by polypyrrole.

Raman spectra of polypyrrole nanotubes/tungsten composites are identical to the Raman spectrum of polypyrrole nanotubes regardless of tungsten content (Figure 6b). They exhibit the bands with maxima situated at 1598, 1495, 1379, 1321, 1240, 1082, 1042, and 923 cm^{-1} [30]. The presence of tungsten and methyl orange is not detected in the spectra of nanotubular polypyrrole due to the resonance enhancement of the Raman spectrum of polypyrrole when using the 780 nm laser excitation line. The bands of methyl orange may be observed when using a 532 nm laser excitation line.

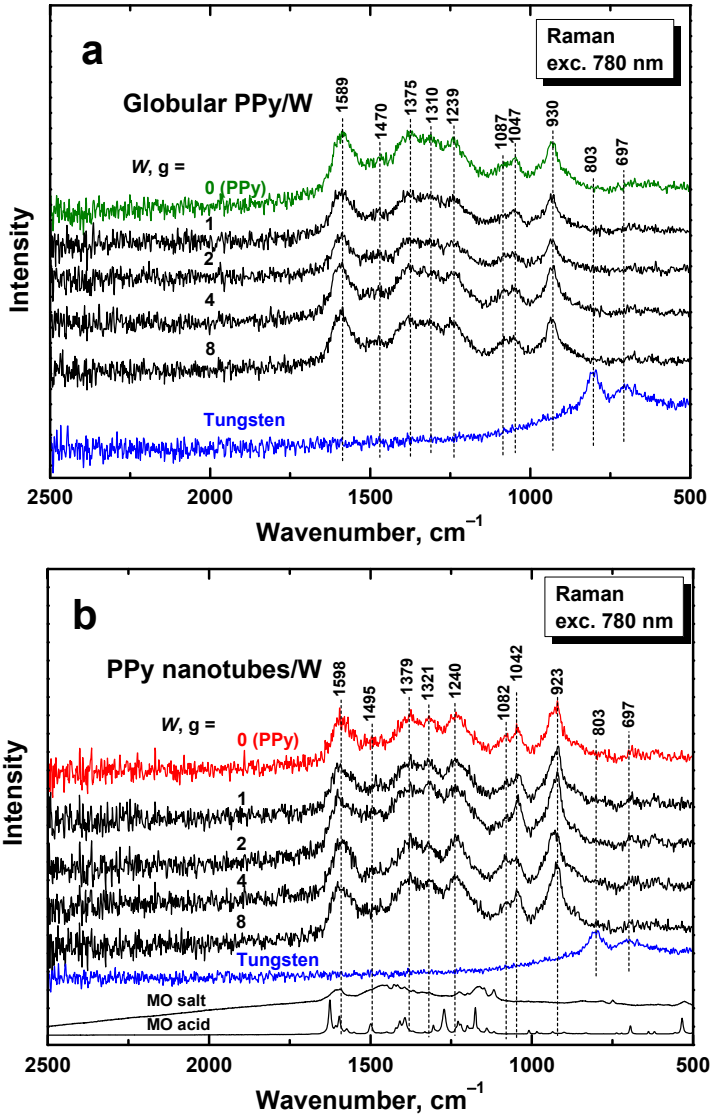

Figure 6. Raman spectra of (**a**) globular and (**b**) nanotubular polypyrrole/tungsten composites depending on mass of tungsten entering the preparation, *W*, per 200 mL of reaction mixture. MO stands for methyl orange dye [29].

3.5. Resistivity

The description of the conducing composites often used the mathematical model of percolation [31–33]. The percolation threshold is a mathematical concept that describes the onset of long-range connectivity in random systems. Let us have a mixture of conducting and nonconducting spheres. When the fraction of conducting spheres is low and they are isolated, the composite is nonconducting. When the volume fraction of conducting objects φ increases, at some moment, the first conducting pathway is produced by conducting spheres. This happens at the so-called percolation threshold, φ_0. When the fraction of conducting objects grows, the conductivity σ increases accordingly and follows the relation $\sigma \sim (\varphi - \varphi_0)^{-x}$ [31,32] and $\sigma = 0$; for fractions below the percolation threshold, $\varphi < \varphi_0$ and x is a parameter. The analogous relation holds for the reciprocal conductivity, i.e., the resistivity $\rho = (\varphi - \varphi_0)^x$. For other systems, the parameter x can be predicted for the various particle shapes.

The percolation concept can be applied to the electrical characterisation of conducting powders. In practical systems, the parameter x depends on the particles' morphology, size distribution, etc. Conducting powders cannot often be compressed to free-standing objects

needed for the routine determination of conductivity, and this parameter has to be obtained after compression at a specified pressure. Needless to say that the conductivity then depends on the applied pressure and it is not a fixed material parameter. In the present experiment, conducting polymer powder was placed into a glass tube and gradually compressed. The degree of compression was monitored by the position of the piston, and the resistivity was determined as a function of applied pressure. Let us imagine that the powder in a tube is placed in a free space. This situation corresponds to the "composite" of powder microparticles at volume fraction φ_1 and dispersed in free space simulating a matrix (Figure 7a). When transferred to ambient conditions, the particles sediment in gravity and the contacts between the particles create the conducting pathways. Such a situation resembles the onset of conduction at percolation threshold at $\varphi_2 = \varphi_0$ (Figure 7b). During the subsequent compression, the volume fraction of conducting phase increases to volume fraction φ_3 and conductivity grows (resistivity decreases). The volume fractions are inversely proportional to the thickness of the sample, d (Figure 7c). The resistivity thus scales as $\rho \sim \varphi^x \sim d^{-x}$, and the double-logarithmic presentations of resistivity dependence on sample thickness are expected to be linear.

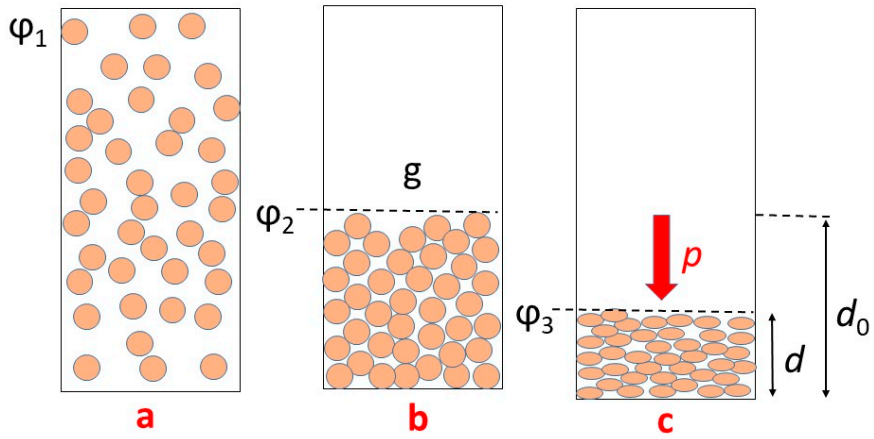

Figure 7. (**a**) The system of conducting particles dispersed in free space is nonconducting due to the absence of sufficient contacts between particles. (**b**) As they sediment under ambient gravity, they contact and create the conducting pathways, and the system becomes conducting. (**c**) After compression by external pressure p, the fraction of components participating in conduction increases and the overall conductivity grows.

The above model was applied in the present case to the powders of individual composite components, polypyrrole and tungsten (Figure 8). Physicists prefer to report the electrical properties in terms of resistivity, while material scientists prefer its reciprocal value, the conductivity. The authors sometimes switch between these two possibilities and apologise to the readers for this inconvenience.

Both types of polypyrrole, globular and nanotubular, well satisfy the linearity of double-logarithmic dependence of resistivity on the sample thickness, i.e., on the degree of compression, respectively. This means that electrical properties depend on the degree of compression, and a single value of conductivity/resistivity cannot be assigned to these materials unless the compression or applied pressure are specified at the same time. The plots also demonstrate the well-known fact that polypyrrole nanotubes have lower resistivity than the globular form. The behaviour of metallic tungsten behaviour is more complex. The nonlinearity of the plot may due to the contact resistances between the individual particles that would be dependent on the degree of compression (Figure 8).

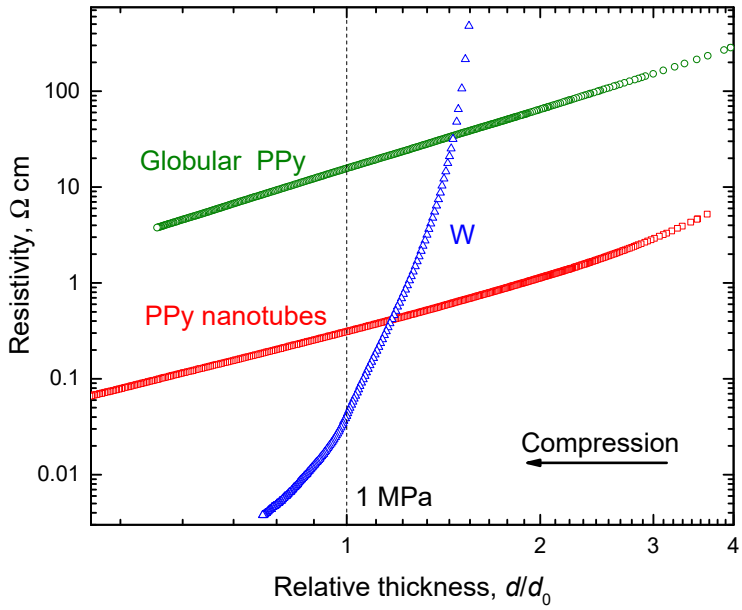

Figure 8. The dependence of resistivity on compression, i.e., on the relative sample thickness d/d_0, where d_0 is the thickness at 1 MPa pressure, for the individual components.

In the next step, the similar dependences of the composites, i.e., polypyrrole-coated tungsten particles, were characterised (Figure 9). At the first impression, it may be surprising that the introduction of conducting metal particles into semiconducting polypyrrole has low, even if any, effect on the resistivity. This is explained as follows: tungsten cores are coated with a polypyrrole shell (Figure 2). When compressed (Figure 7), the tungsten microparticles become embedded in a matrix of polypyrrole and their mutual contact is prevented. The tungsten particles cannot thus create conducting pathways; they find themselves below the percolation threshold. Therefore, they do not contribute to the overall composite conductivity, which is determined exclusively by polypyrrole matrix. Both types of polypyrrole coatings of tungsten, globular and nanotubular, display the same trends (Figure 9a,b); only those with nanotubes have lower resistances.

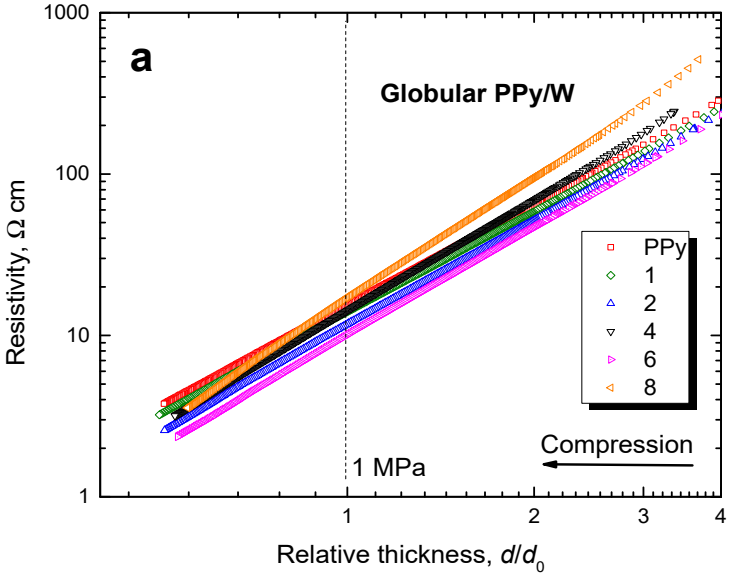

Figure 9. *Cont.*

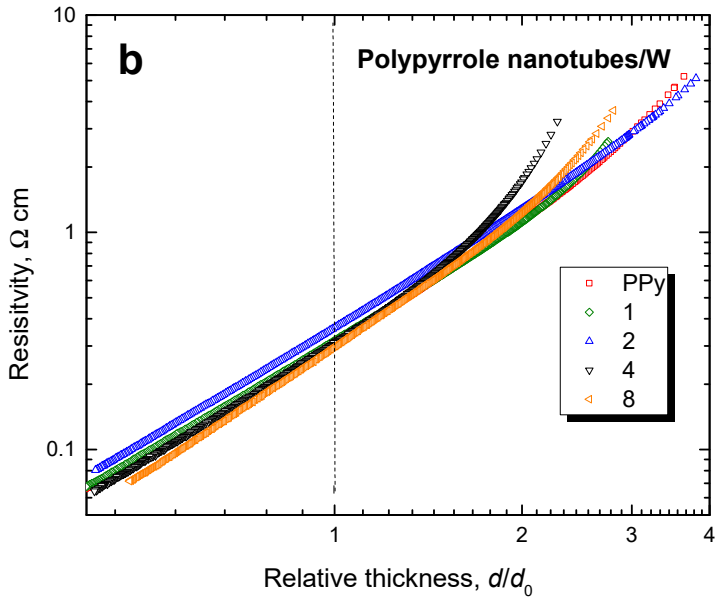

Figure 9. The dependence of resistivity on compression, i.e., on the relative sample thickness d/d_0, where d_0 is the thickness at 1 MPa pressure for the composites with (**a**) globular polypyrrole and (**b**) polypyrrole nanotubes. Numbers 1–8 refer to the grams of W entered per 200 mL of reaction mixture (Table 1).

The above interpretation is further supported by the unexpected observation that the composites with higher tungsten metal content have even somewhat lower conductivity (i.e., higher resistivity). This is due to the fact that conducting tungsten particles behave as a nonconducting filler (in practice ca. $<10^{-6}$ S cm^{-1}), which decreases the volume fraction of conducting polypyrrole phase and, consequently, the overall composite conductivity. The analogous behaviour has been found with polypyrrole-coated microparticles of manganese–zinc ferrite [28].

According to the available information, tungsten metal is stable with respect to oxidation under acidic conditions. In principle, however, the passivation of the metal surface cannot be ruled out. If present, however, it could affect the electrical properties at the polypyrrole/tungsten interface and increase the apparent resistivity of the filler.

3.6. Mechanical Properties

The present experimental setup provides also information on the mechanical properties of powders, i.e., how easily the powder yields to the applied pressure (Figure 10). The dependences of the relative thickness on the pressure are close to linear for all composite components. The steeper they are, the fluffier and easier to compress the material is. The absolute values of slopes were 0.121 for tungsten, 0.276 for globular polypyrrole, and 0.384 for polypyrrole nanotubes and can be regarded as parameters characterising the material with respect to its specific morphology.

When applied to the composites with tungsten, there is, again, only a marginal effect of tungsten filler. All composites behave similarly to neat polypyrrole (Figure 11). At higher tungsten contents, less steep dependences are observed, indicating some material stiffening at high pressures.

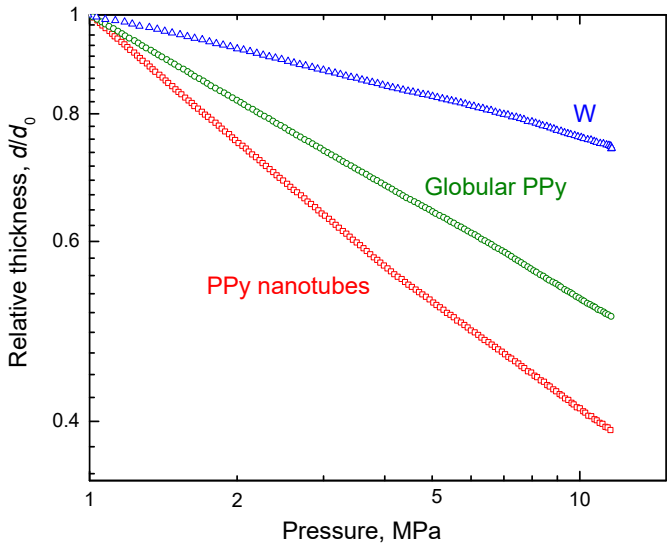

Figure 10. The relative sample thickness, d/d_0, with respect to the thickness d_0 at 1 MPa pressure as a function of applied pressure for individual components.

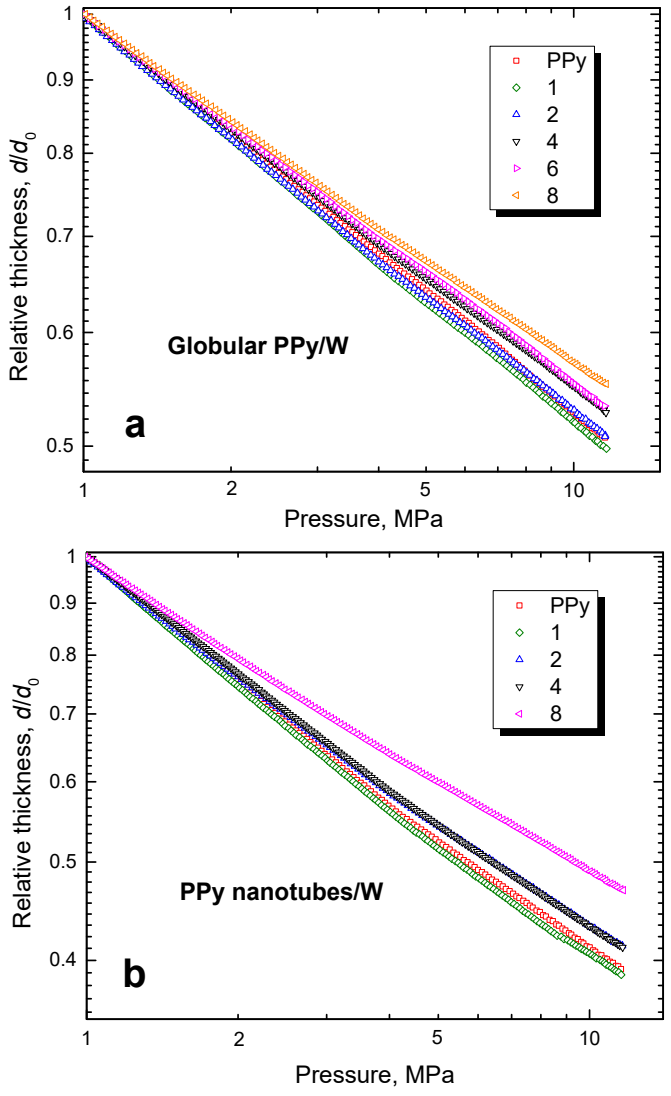

Figure 11. The relative sample thickness, d/d_0, with respect to the thickness d_0 at 1 MPa pressure as a function of applied pressure for the tungsten composites with (**a**) globular polypyrrole and (**b**) polypyrrole nanotubes. Numbers 1–8 refer to the grams of W entered per 200 mL of reaction mixture (Table 1).

3.7. Pressure Dependences of Resistivity

For some applications, the presentation in terms of resistivity dependence on pressure may be of interest. For both polypyrrole components, the double-logarithmic plots are linear, with similar slopes 0.679 and 0.687 for globular and nanotubular polypyrrole, respectively (Figure 12). As mentioned above, the behaviour of tungsten alone is more complex.

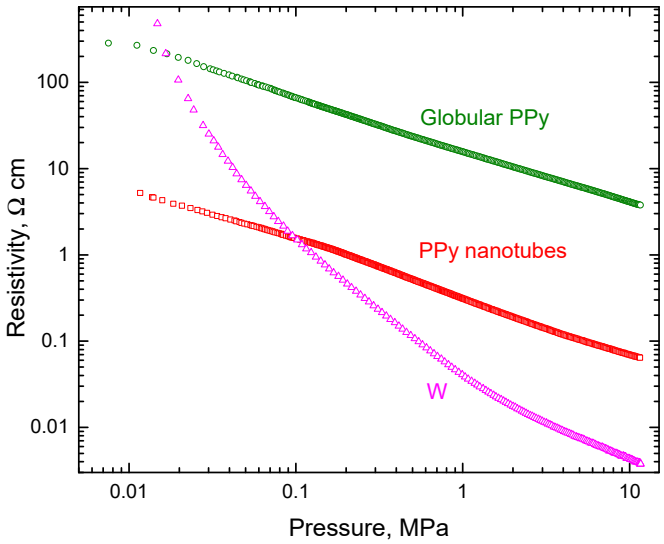

Figure 12. Resistivity of individual composite components as a function of applied pressure.

The electrical properties of composite are shown for the sake of completeness (Figure 13), just illustrating again the dominating role of polypyrrole. The composites with nanotubes have lower resistivity compared with globular polypyrrole but, otherwise, the responses to the applied pressure are similar.

When the powders can be compressed to yield free-standing pellets, the routine determination of conductivity can be carried using the four-point van der Pauw setup. The conductivity of globular polypyrrole under 10 MPa pressure and that determined with a pellet prepared at 527 MPa are close to each other (Table 2). With polypyrrole nanotubes, however, the pellets had about twice higher conductivity than under 10 MPa compression. This means that the conductivity of powders should always refer to the applied pressure. The results again confirm that the presence of tungsten has a negligible effect on the electrical properties of its core–shell composites with polypyrrole.

Table 2. Conductivity (S cm^{-1}) of globular polypyrrole and polypyrrole nanotubes and composites with tungsten under 10 MPa pressure or on a pellet prepared under 527 MPa pressure.

W Content [a]	Globular PPy		PPy Nanotubes	
	10 MPa	Pellet (527 MPa)	10 MPa	Pellet (527 MPa)
0	0.244	0.288	14.4	28.4
1	0.283	0.285	14.5	34.2
2	0.353	0.418	11.5	19.6
4	0.256	0.347	15.0	36.1
8	0.254	0.335	12.8	27.4

[a] Numbers 0–8 refer to the grams of tungsten entered per 200 mL of reaction mixture (Table 1). The higher the number, the higher the content of tungsten in the composite.

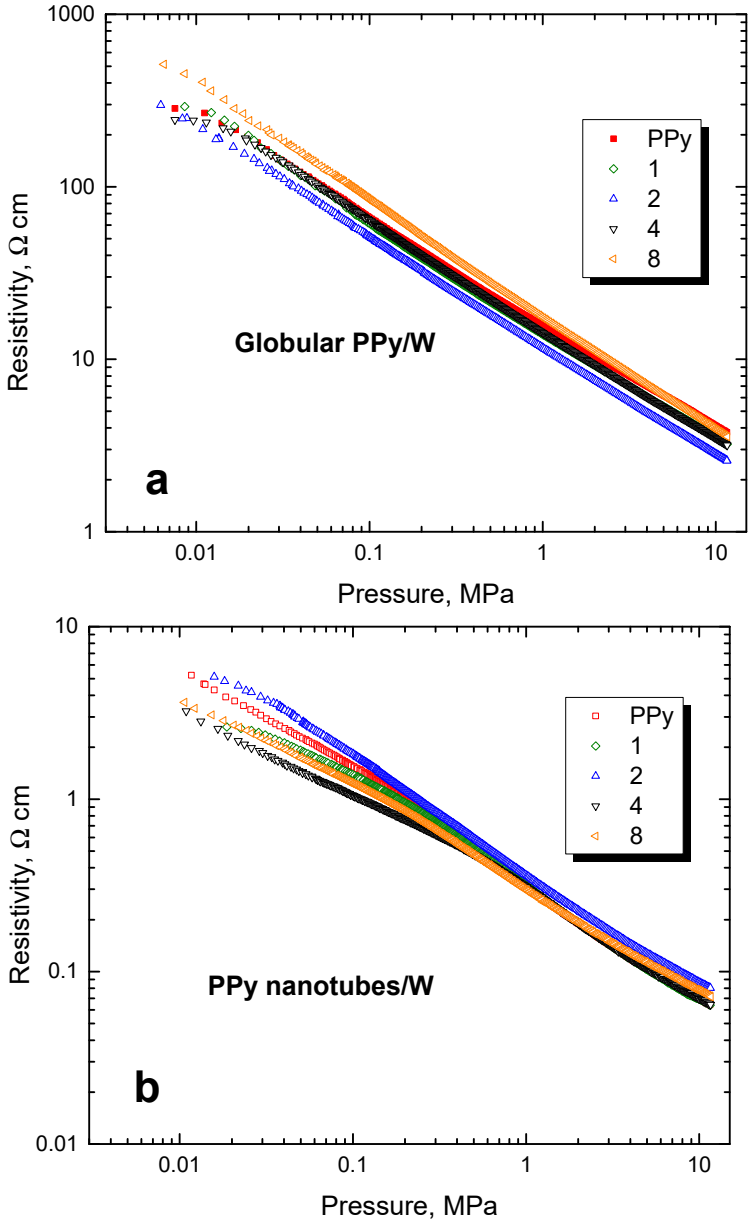

Figure 13. Resistivity of tungsten composites with (**a**) globular polypyrrole or (**b**) polypyrrole nanotubes as a function of applied pressure. Numbers 1–8 refer to the grams of W entered per 200 mL of reaction mixture (Table 1).

4. Conclusions

Core–shell polypyrrole-coated tungsten microparticles are composites combining an organic semiconductor with a metallic conductor. When characterised as powders, the electrical properties, viz. DC resistivity/conductivity, depend on the applied pressure. The composite conductivity is determined by the polypyrrole matrix. Despite its metallic conduction, tungsten microparticles behave as a nonconducting filler, and they do not contribute to the composite conductivity. The conductivity of the composites based on polypyrrole nanotubes was up to 12–15 S cm^{-1} at 10 MPa, i.e., higher than 0.24–0.35 S cm^{-1} for globular polypyrrole, regardless of the tungsten content.

Author Contributions: J.S.: Conceptualisation, Writing—Review and Editing. M.J.: Methodology, Data Curation. M.T.: Validation, Methodology. J.P.: Investigation, Data Curation. All authors have read and agreed to the published version of the manuscript.

Funding: This work was supported by the Ministry of Education, Youth and Sports of the Czech Republic (DKRVO RP/CPS/2024-28/005) and Technology Agency of the Czech Republic (TK03030157).

Data Availability Statement: No data available.

Conflicts of Interest: The authors declare that they have no competing interests that could have appeared to influence the work reported in this paper.

References

1. Liao, Z.W.; Zoumhani, O.; Boutry, C.M. Recent advances in magnetic polymer composites for bioMEMS: A review. *Materials* **2023**, *16*, 3802. [CrossRef]
2. Macdonald, M.; Zhitomirsky, I. Pseudocapacitive and magnetic properties of $SrFe_{12}O_{19}$-polypyrrole composites. *J. Compos. Sci.* **2024**, *8*, 351. [CrossRef]
3. Wang, G.P.; Zhang, L.; Zhang, J.J. A review of electrode materials for electrochemical supercapacitors. *Chem. Soc. Rev.* **2012**, *41*, 797–828. [CrossRef] [PubMed]
4. Soares, B.G.; Barra, G.M.O.; Indrusiak, T.J. Conducting polymeric composites based on intrinsically conducting polymers as electromagnetic interference shielding/microwave absorbing materials—A review. *J. Compos. Sci.* **2021**, *5*, 173. [CrossRef]
5. Ul Hoque, M.I.; Holze, R. Intrinsically conducting polymer composites as active masses in supercapacitors. *Polymers* **2023**, *15*, 730. [CrossRef] [PubMed]
6. Nedjar, L.; Mekki, A.; Sayah, Z.B.D.; Cherfa, M.C.; Lounes, R.A.; Manseri, A.; Durastanti, J.F.; Mekhalif, Z. Towards an efficient p-n heterojunction in ternary composite material based polypyrrole, metal oxide and surface functionalized graphene for thermoelectric properties enhancement. *Synth. Met.* **2023**, *298*, 117427. [CrossRef]
7. Filipescu, M.; Dobrescu, S.; Bercea, A.I.; Bonciu, A.F.; Marascu, V.; Brajnicov, S.; Palla-Papavlu, A. Polypyrrole-tungsten oxide nanocomposite fabrication through laser-based techniques for an ammonia sensor: Achieving room temperature operation. *Polymers* **2024**, *16*, 79. [CrossRef]
8. Rabia, M.; Aldosari, E.; Elsayed, A.M.; Sanna, A.; Farid, O. Highly porous network of tungsten (VI) oxide-iodide/polypyrrole nanocomposite photocathode for the green hydrogen generation. *Opt. Quant. Electron.* **2024**, *56*, 1068. [CrossRef]
9. Li, Y.; Zhao, Z.; Zhang, J.W.; Chen, Z.; Liu, X.; Wang, K.L.; Sobolev, A.V.; Savilov, S.V.; Chen, M.H. High pseudocapacitance electrode enabled by heterovalent doping and surface coating for rapid charge storage. *Surf. Coat. Technol.* **2024**, *476*, 130169. [CrossRef]
10. Cogal, S.; Cogal, G.C.; Mičušík, M.; Kotlár, M.; Omastová, M. Cobalt-doped WSe_2@conducting polymer nanostructures as bifunctional electrocatalysts for overall water splitting. *Int. J. Hydrogen Energy* **2024**, *49*, 689–700. [CrossRef]
11. Liu, Y.; Wei, H.J.; Wang, C.; Wang, F.; Wang, H.C.; Zhang, W.H.; Wang, X.F.; Yan, C.L.; Kim, B.H.; Ren, F.Z. Nitrogen-doped carbon coated WS_2 nanosheets as anode for high-performance sodium-ion batteries. *Front. Chem.* **2018**, *6*, 236. [CrossRef] [PubMed]
12. Stejskal, J.; Acharya, U.; Bober, P.; Hajná, M.; Trchová, M.; Mičušík, M.; Omastová, M.; Pašti, I.; Gavrilov, N. Surface modification of tungsten disulfide with polypyrrole for enhancement of the conductivity and its impact on hydrogen evolution reaction. *Appl. Surf. Sci.* **2019**, *492*, 497–503. [CrossRef]
13. Sunilkumar, A.; Manjunatha, S.; Machappa, T.; Chethan, B.; Ravikiran, Y.T. A tungsten disulphide-polypyrrole composite-based humidity sensor at room temperature. *Bull. Mater. Sci.* **2019**, *42*, 271. [CrossRef]
14. Hsiao, P.F.; Anbazhagan, R.; Tsai, H.C.; Krishnarnoorthi, R.; Lin, S.J.; Lin, S.Y.; Lee, K.Y.; Kao, C.Y.; Chen, R.S.; Lai, J.Y. Fabrication of electroactive polypyrrole-tungsten disulfide nanocomposite for enhanced in vivo drug release in mice skin. *Mater. Sci. Eng. C* **2020**, *107*, 110330. [CrossRef] [PubMed]
15. Sunilkumar, A.; Manjunatha, S.; Ravikiran, Y.T.; Revanasiddappa, M.; Prashantkumar, M.; Machappa, T. AC conductivity and dielectric studies in polypyrrole wrapped tungsten disulphide composites. *Polym. Bull.* **2021**, *79*, 1391–1407. [CrossRef]
16. Selvam, S.; Yim, J.H. Multifunctional supercapacitor integrated sensor from Oyster and Cicada derived bio-ternary composite: Vanillin/caffeine detections in beverages. *J. Energy Storage* **2022**, *45*, 103791. [CrossRef]
17. Kozma, M.; Bissessur, R.; Gao, B.W.; Dahn, D.C. Exfoliated tungsten disulfide-polypyrrole nanocomposites. *J. Inorg. Organomet. Polym. Mater.* 2024; *early access*. [CrossRef]
18. Selvam, S.; Jo, Y.H.; Chan, A.D.; Cumming, M.; Jordan, M.; Khadka, R.; Yim, J.H. Biocompatible supercapacitor engineered from marine collagen impregnated with polypyrrole and tungsten disulfide. *J. Energy Storage* **2024**, *96*, 112735. [CrossRef]
19. Mohan, V.V.; Rakhi, R.B. WS_2/conducting polymer nanocomposite-based flexible and binder-free electrodes for high-performance supercapacitors. *Elecrochim. Acta* **2024**, *498*, 144657. [CrossRef]
20. Arslantürk, G.; Ugraskan, V. Thermoelectric properties investigation of tungsten carbide-filled poly(vinyl alcohol)/polypyrrole ternary composites. *Polym. Plast. Technol. Mater.* **2024**, *63*, 151–160. [CrossRef]
21. Minisy, I.M.; Gupta, S.; Taboubi, O.; Acharya, U.; Bober, P. Polypyrrole/tungsten carbide nanocomposites for electrochemical applications. *ACS Appl. Polym. Mater.* **2024**, *6*, 8244–8253. [CrossRef]

22. Turek, W.; Lapkowski, M.; Stolarczyk, A.; Debiec, J. EPR and XPS measurements of polymeric catalysts doped with heteropolyacids in oxygen adsorption studies. *Appl. Surf. Sci.* **2005**, *252*, 801–806. [CrossRef]
23. Yasami, S.; Mazinani, S.; Abdouss, M. Developed composites materials for flexible supercapacitors electrode: "Recent progress & future aspects". *J. Energy Storage* **2023**, *72*, 108807. [CrossRef]
24. Stejskal, J.; Jurča; Vilčáková, J.; Trchová, M.; Kolská, Z.; Prokeš, J. Conducting polypyrrole silicotungstate deposited on macroporous melamine sponge for electromagnetic interference shielding. *Mater. Chem. Phys.* **2023**, *293*, 126707. [CrossRef]
25. Tyagi, N.; Singh, M.K.; Khanuja, M. Synergistic effect of polypyrrole modified WS_2 nanosheets on visible light assisted catalysis for the removal of chromium (VI) and humic acid. *Mater. Res. Bull.* **2023**, *163*, 112216. [CrossRef]
26. Tyagi, N.; Ashraf, W.; Mittal, H.; Fatima, T.; Khanuja, M.; Singh, M.K. A facile synthesis of ternary hybrid nanocomposite of WS_2/ZnO/PPy: An efficient photocatalyst for the degradation of chromium hexavalent. *Dye. Pigment.* **2023**, *210*, 110998. [CrossRef]
27. Muthumeenal, A.; Rethinam, A.J.; Nagendran, A. Sulfonated polyethersulfone based composite membranes containing heteropolyacids laminated with polypyrrole for electrochemical energy conversion devices. *Solid State Ion.* **2016**, *296*, 106–113. [CrossRef]
28. Jurča, M.; Munteanu, L.; Vilčáková, J.; Stejskal, J.; Trchová, M.; Prokeš, J.; Křivka, I. Core–shell inorganic/organic composites composed of polypyrrole nanoglobules or nanotubes deposited on MnZn ferrite microparticles: Electrical and magnetic properties. *J. Compos. Sci.* **2024**, *8*, 373. [CrossRef]
29. Stejskal, J.; Trchová, M. Conducting polypyrrole nanotubes: A review. *Chem. Pap.* **2018**, *72*, 1563–1595. [CrossRef]
30. Trchová, M.; Stejskal, J. Resonance Raman spectroscopy of conducting polypyrrole nanotubes: Disordered surface versus ordered body. *J. Phys. Chem. A* **2018**, *122*, 9298–9306. [CrossRef]
31. Zallen, R.; Scher, H. Percolation on a continuum and localization–delocalization transition in amorphous semiconductors. *Phys. Rev. B-Solid State* **1971**, *4*, 4471–4476. [CrossRef]
32. Křivka, I.; Prokeš, J.; Tobolková, E.; Stejskal, J. Application of percolation concepts to electrical conductivity of polyaniline-inorganic salt composites. *J. Mater. Chem.* **1991**, *9*, 2425–2428. [CrossRef]
33. Oskouyi, A.B.; Sundararaj, U.; Mertiny, P. Tunneling conductivity and piezoresistivity of composites containing randomly dispersed conductive nano-platelets. *Materials* **2014**, *7*, 2501–2521. [CrossRef]